UNIVERSITÀ DI SIENA 1240

USiena

Intermolecular Modes Between LH2 Bacteriochlorophylls and Protein Residues; the Effect on the Excitation Energies

This is the peer reviewed version of the following article:

Original:

Anda, A., DE VICO, L., Hansen, T. (2017). Intermolecular Modes Between LH2 Bacteriochlorophylls and Protein Residues; the Effect on the Excitation Energies. JOURNAL OF PHYSICAL CHEMISTRY. B, CONDENSED MATTER, MATERIALS, SURFACES, INTERFACES & BIOPHYSICAL, 121(22), 5499-5508 [10.1021/acs.jpcb.7b02071].

Availability:

This version is availablehttp://hdl.handle.net/11365/1007497 since 2017-06-13T18:48:00Z

Published:

DOI:10.1021/acs.jpcb.7b02071

Terms of use:

Open Access

The terms and conditions for the reuse of this version of the manuscript are specified in the publishing policy. Works made available under a Creative Commons license can be used according to the terms and conditions of said license.
For all terms of use and more information see the publisher's website.

(Article begins on next page)

10 April 2024

Intermolecular Modes between LH2 Bacteriochlorophylls and Protein Residues; the Effect on the Excitation Energies

André Anda,[†] Luca De Vico,[*,†,‡] and Thorsten Hansen[*,†]

Department of Chemistry, H. C. Ørsted Institute, University of Copenhagen, Universitetsparken 5, DK-2100 Copenhagen, Denmark, and Department of Biotechnology, Chemistry and Pharmacy, University of Siena, via Aldo Moro 2, 53100 Siena, Italy

E-mail: Luca.DeVico@unisi.it; thorsten@chem.ku.dk

Phone: +39 0577 234281; +45 22 29 57 28.

Abstract

Light-harvesting system 2 (LH2) executes the primary processes of photosynthesis in purple bacteria; photon absorption and energy transportation to the reaction centre. A detailed mechanistic insight into these operations is obscured by the complexity of the light-harvesting systems, particularly by the chromophore-environment interaction. In this work, we focus on the effects of the protein residues that are ligated to the bacteriochlorophylls (BChls), and construct potential energy surfaces of the ground and first optically-excited state for the various BChl-residue systems, where we in each case consider two degrees of freedom in the intermolecular region. We find that the excitation energies are only slightly affected by the

*To whom correspondence should be addressed
†Copenhagen University
‡University of Siena

considered modes. In addition, we see that axial ligands and hydrogen-bonded residues have opposite effects on both excitation energies and oscillator strengths, by comparing to the isolated BChls. Our results indicate that only a small part of the chromophore-environment interaction can be associated with the intermolecular region between a BChl and an adjacent residue, but that it may be possible to selectively raise or lower the excitation energy at the axial and planar residue positions, respectively.

Introduction

The initial steps of photosynthesis are the capture of sunlight and subsequent delivery of the absorbed solar energy to the reaction centre, where charge separation takes place. These tasks are performed by the photosynthetic light-harvesting systems which consist of chromophores held in place by a protein scaffold. The exact mechanisms which make possible the highly efficient[1–6] energy transfer processes in these systems are not fully understood, but are a topic of intense research.

The many degrees of freedom activated at biological temperatures make for a highly fluctuating environment. It therefore came as a surprise when evidence of sustained quantum dynamics was found in photosynthetic light-harvesting systems.[7,8] The role of quantum coherent motion in energy transfer and charge separation is still one of the big open questions in the field; however, in recent years, the debate has been gravitating towards the interaction between the photoactive chromophores and the noisy environment. It is now known that the environment interaction plays a decisive and potentially constructive part in the energy transfer. So-called noise-assisted transport is the idea that the interplay of the relevant system with its fluctuating environment opens up relaxation pathways which direct the energy towards a sink, which in some cases boosts the transfer rate compared to the fully coherent situation.[9,10]

To understand the detailed mechanisms of photosynthetic light-harvesting, theoretical

models need to be able to simulate the dynamics in the experimental spectra obtained using ultrafast spectroscopies. Our previous paper demonstrated that highly accurate multireference quantum chemical methods can be used to compute input parameters for the theoretical models.[11] In particular, we calculated excitation energies and transition dipole moments for all bacteriochlorophylls *a* (BChls) in light-harvesting system 2 (LH2). Along with the resonant coupling terms, these parameters make up the backbone of the model. However, realistic models also need an accurate description of the interaction with the environment.[12] Usually, this information is contained in the spectral density, which is the density of bath modes weighted by the square of their couplings to the system. In most theoretical methods, the spectral density enters as a perturbation, but it has also been employed for non-perturbative methods.[13] Alternatively, specific interactions with the environment can be included explicitly as individual degrees of freedom.

The growing body of work on the chromophore-environment interaction has seen a wide fan of different approaches.[14] Perhaps the most common approach is a classical treatment of the environment,[15–21] either in form of continuum models or point-charges models. The effect of the environment can then be elucidated by comparing different partitionings of an inner quantum region and an outer classical region, or by performing a molecular dynamics simulation and Fourier transforming the autocorrelation function of the site-energy fluctuations to obtain the spectral density. An immediate disadvantage with these methods is the low accuracy and neglect of quantum contributions. A similar, but fully quantum mechanical, approach is to use subsystem TDDFT, which divides the whole system into smaller fragments, thus allowing systems with more than 1000 atoms to be treated.[22–24]

An alternative strategy to the molecular-dynamics based method, is to calculate the spectral density directly using normal mode analysis.[25,26] The spectral density gives information on the dynamical evolution due to the coupling to the environment, whereas systematically including larger environments will give the static contribution to the energy. While both pieces of information may be sufficient to model experimental spectra, a complete under-

standing of the role of the environment also requires the conformational changes induced by the environment to be known. Such geometrical variations may be quantified using normal-coordinate structural decomposition and subsequently correlated to the site energies, thus revealing the most important conformational changes.[27]

Theoretical methods have been the preferred choice for extracting energies and couplings from within light-harvesting complexes, but experimental methods are now emerging. The experimental techniques generally require a bottom-up approach to isolate specific energies or couplings. Some examples include a comparison of single chlorophylls with and without an axial ligand[28] and a study of a BChl dimer.[29] However, top-down approaches, such as comparing structures and spectra of closely related pigment-protein complexes can give invaluable clues to the underlying mechanisms.[30]

In this work, we take a separate approach as we narrow our study to the intermolecular regions between BChls and adjoining protein residues in LH2. We map out potential energy surfaces (PESs) for the ground state and optically-accessible excited state of two-dimensional intermolecular modes where one coordinate is associated with the BChl and the other with either an axial ligand or a hydrogen bonded (H-bonded) residue. To highlight the smaller differences between the groung and excited state, we also plot the excitation energy surfaces (EESs). Subsequently, we perform a vibrational analysis to investigate the interplay of nuclear and electronic motion.

The BChls in LH2 are arranged in two parallel rings, one containing 9 BChls, the other consisting of 18 BChls, see Figure 1. The closer packing in the latter causes a redshift of the excitation energy, resulting in an absorption band at around 850 nm, while the other ring absorbs at about 800 nm. The rings are named B850 and B800 accordingly.

Computational work on the LH2 system is aided by the high degree of symmetry. The crystal structure[31] has C_3 symmetry, which allowed us to consider only one of the three subunits in our previous work.[11] The B800 BChls in this subunit are not identical, but they are sufficiently similar that we, in this work, only consider one such chromophore with its

adjacent protein residues, which are always the same; arginine and a carboxylated methionine (henceforth only referred to as methionine). The B850 BChls are alternating between two different orientations, which we designate the BChl α and the BChl β. In addition, they toggle between having a tyrosine and a tryptophan residue in the immediate environment. We therefore need to study both the α and the β monomers. Both monomers are also ligated to a histidine residue.

Tyrosine/tryptophan/arginine links the apoprotein and the B850 α/B850 β/B800 BChl via a H-bond between an acetyl group on the BChl and a hydroxyl/amine/amine on the residue. It has previously been proposed that the rotation around the acetyl group is a mechanism to tune the site-energy.[11,32,33]

Histidine/methionine on the other hand is positioned above the macrocycle ring, and may interact with the magnesium in the BChl. This interaction can possibly redistribute charge[34–36] or pull the Mg slightly out of the plane. Figure 2 shows the specific residues and BChl units studied in this work.

How the different mechanisms affect the excitation energies, and in turn, the energy transfer, is not fully understood. However, a comprehensive study[15] on the environmental effects in the Fenna-Matthews-Olson[37,38] (FMO) pigment-protein complex, found that interactions between the BChl with the axial ligand and with the H-bonded residues were responsible for tuning the site-energies. These modulations were attributed mainly to electrostatic interactions, but also to short-range quantum interactions. Also the experimental work[28] on a chlorophyll with an axial ligand found the axial ligand to have a strong impact on the absorption, although it is unclear whether this effect was purely electrostatic, since the ligand was charged.

Concerning the H-bonded residues, it has been known for a long time that altering the primary structure of the apoproteins leads to substantial shifts in the absorption band and energy transfer properties. This occurs naturally in LH3[32] but it has also been demonstrated using site-directed mutagenesis on LH2.[39] It was argued that changes in the H-bonding pat-

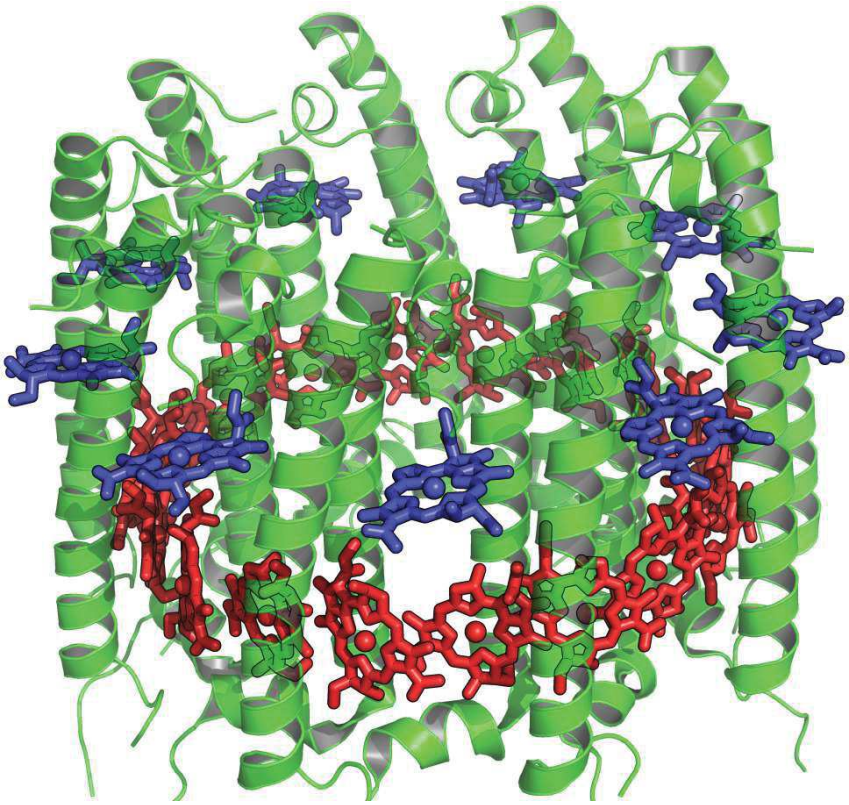

Figure 1: Light Harvesting System 2 constituted by a protein scaffold (green) and two rings of bacteriochlorophylls; the B850 ring (red) containing 18 BChls, and the B800 ring (blue) containing 9 BChls. Carotenoids have been omitted for clarity.

terns (or lack of H-bonds in LH3) between the BChls and the protein affected the conformation of the C_3 acetyl groups, which in turn shifted the excitation energy. However, in a recent, more detailed study of water-soluble chlorophyll binding proteins, modifications of the H-bonding to a nearby tryptophan residue brought on ring deformation of the chlorophyll macrocycle which could explain the observed spectral shift.[30]

The computational study of intermolecular BChl-protein modes presented herein will provide new insight into the fine-tuning of BChl site energies in LH2. By isolating the degrees of freedom to the intermolecular region, we obtain a clearer picture of the dynamics at the points of contact between the BChl and the protein, and can give an estimate of how much of the total effect of the environment is captured in this region.

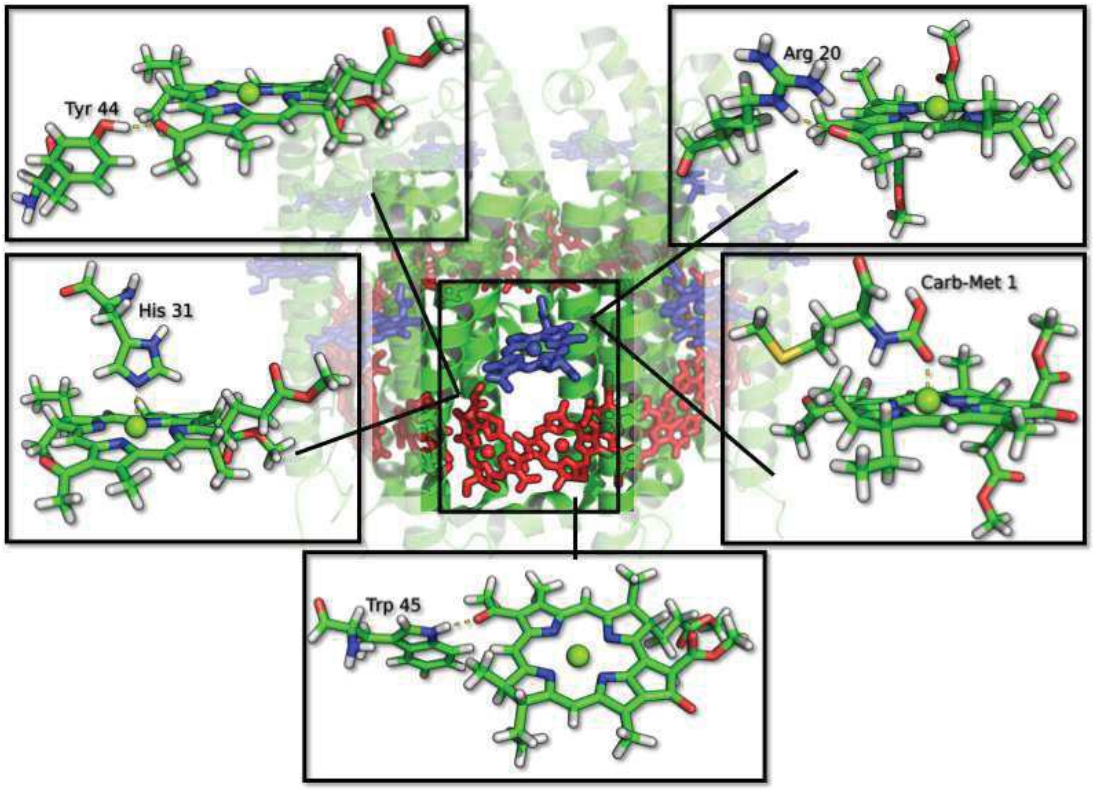

Figure 2: Background: Light Harvesting System 2 as seen in Figure 1. Middle: BChl units 304, 305 and 308 are chosen as representative units to study the effect of proximate protein residues. Clockwise from the top left: The BChl-residue complexes studied herein are BChl-tyrosine, BChl-arginine, BChl-carb. methionine, BChl-tryptophan and BChl-histidine, with residue numbers 44, 20, 1, 45 and 31, following the numbering in protein database file 1NKZ.

Computational Methods

Structures preparation

The structure preparation procedure starting with the crystal structure[31] is detailed in our previous paper, the new feature here is simply that the residue is included and truncated at the peptide bond as indicated by Figure 3, and that the mentioned degrees of freedom are altered. Note, however, that we have completely neglected the electrostatics of the environment on the grounds that the BChl units are embedded in the apolar part of the protein and hence we do not expect substantial electrostatic effects on the BChl excitation energies, as seen previously.[? ?] While ignoring the electrostatic effects introduces some uncertainty concerning the energies, we are mostly interested in the dynamics of the considered modes, where we believe the effect of the electrostatic environment is more or less the same on all configurations. In other words, we assume the electrostatics to only shift the surfaces up or down, not to change their shapes.

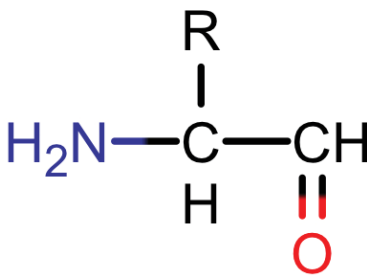

Figure 3: Structure of a generic, truncated amino acid showing how the peptide bond is saturated. R indicates the residue side chain, which in our study can be tyrosine, tryptophan, histidine, arginine and (neutral or negative) methionine.

In case the investigated mode is some concerted motion, we will for each of the five residues consider two degrees of freedom. For tyrosine, tryptophan and arginine we investigate the joint effect of the dihedral angle of the acetyl moiety and the shuttling of the proton in the H-bond. For histidine we will consider the movement of the Mg and the histidine relative to the original crystal structure. For methionine we performed a vibrational frequency analysis (see the supplementary information) and found a dominating stretching mode on

the carboxylic functional group that we used as one coordinate, while the position of the Mg atom relative to the crystal structure remained the second coordinate. The various modes are depicted in Figure 4.

More specifically for the H-bonded residues, we compute ground- and excited state energies for the grid of configurations defined by the crystal structure with the dihedral angle ranging from -10 degrees to +6 degrees with respect to the starting structure, and the proton in the H-bond displaced -0.4 to 1.1 Å with respect to the starting structure (-0.5 to 1.1 Å in the tyrosine case), but with the hydrogen moved along the straight line connecting the BChl and the residue. Increments are 2 degrees and 0.1 Å, respectively.

For the BChl-histidine complex, we first defined a vector on the straight line from Mg to the closest N on histidine, and then displaced both Mg and the whole of histidine independently along the vector in the intervals [-0.3,0.3] and [-0.5,0.5], with increments of 0.05 and 0.1 Å, respectively.

For the BChl-methionine calculations, we defined a vector on the straight line between Mg and the closest O on methionine for all configurations. The Mg was moved along this vector, in the same increments as for the BChl-histidine calculation, while the eigenvector of the vibrational mode, see supplementary information, was scaled by multiples of 0.05, which meant the nearest O atom moved in steps of approximately 0.033 Å towards the BChl and the nearest C atom moved in steps of approximately 0.19 Å away from the BChl. For the methionine calculations we also repeated the calculations with a negative charge, since the protonation state of this residue is undetermined.

Energy Evaluation

As the method of our previous paper is computationally expensive, we chose to use time-dependent density-functional theory (TD-DFT)[40–42] to map out the surfaces. Some selected configurations were also calculated with MS-RASPT2/2-roots-SA-RASSCF,[43–46] so as to validate the TD-DFT results. Again, we employed the same specifications as in the pre-

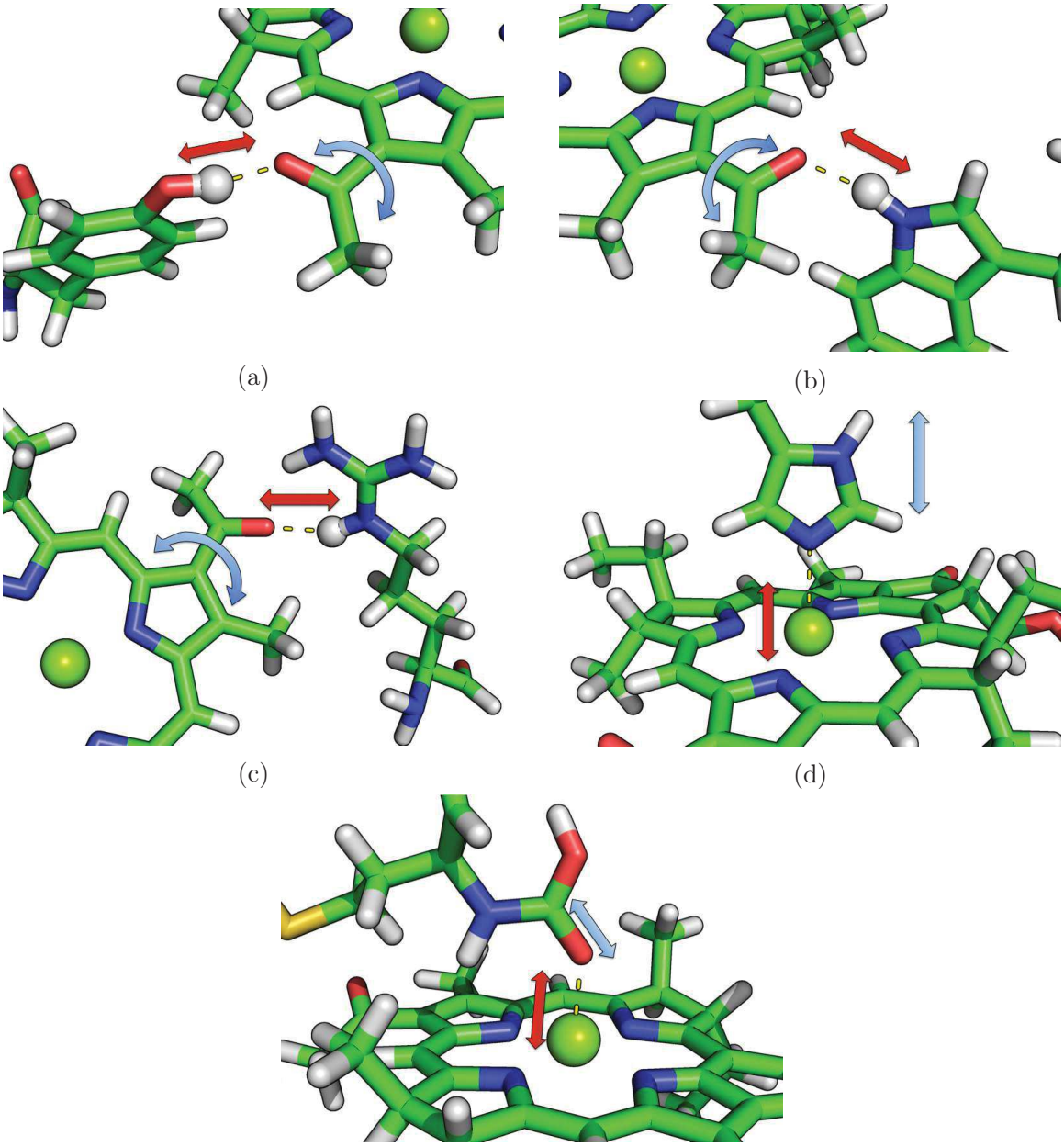

Figure 4: Intermolecular modes between BChls and residues. The considered modes between a) BChl unit 304 and tyrosine, b) BChl unit 305 and tryptophan and c) BChl unit 308 and arginine, are the dihedral angle of the acetyl moiety (blue curved arrow) and the shuttling of the proton in the H-bond (red arrow). For BChl unit 304 with the axial histidine residue in d), we consider the movements of the Mg atom and the entire truncated histidine along their displacement vector (indicated by the yellow dashed line). In e), the Mg atom of BChl unit 308 is also moved along the vector defined by the nearest O on methionine and Mg itself, but on the methionine we consider a vibrational mode where the nearest O and the adjacent C atom contract or move apart. More on this vibrational mode can be found in the supplementary information.

vious article, namely an ANO-RCC double zeta basis set,[47] same active space (26 active electrons, 11 orbitals in RAS1, 4 in RAS2, 10 in RAS3, 3 holes and excitations), using MOLCAS [version 7.8][48] and some features from the developer code [version 8.1] to speed up the calculation.[49] Hydrogen atoms were added using the program Avogadro,[50] and their positions optimized with PM6[51] using Gaussian version 09.[52] Full cartesian coordinates of the considered molecular systems are given as supplementary information.

For all TD-DFT calculations, we employed the LS-DALTON quantum chemistry package[53] [version 2015.0]. We used the 6-311+G* basis set,[54–56] with the df-def2 auxiliary basis.[57] We employed the PBE0 exchange-correlation functional,[58] as this has been found to yield low errors compared to a benchmark DFT/MRCI method, when calculating excitation energy differences among FMO bacteriochlorophylls.[59] For evaluating integrals, we utilized density-fitting for the Coulomb contribution, so as to speed up the calculations, together with a threshold of 10^{-15}.For the density optimisation procedure, we used a dynamic SCF convergence threshold (.COVNDYN). Due to the relatively large size of the molecule, we used a trilevel starting guess and the Augmented Rothaan-Hall method for density optimisation together with a reduced space solver based Davidson's algorithm.[60] We calculated 5 excitation energies, in order to find the relevant excited state corresponding to an optical transition with a large oscillator strength.

The energy evaluation procedure described above was chosen after trial and error showed it was the best compromise for all considered systems. However, some calculations did not converge, which resulted in holes in some of the surfaces.

Vibrational Analysis

The PESs provide information on the nuclear motion and how vibrations can couple to electronic transitions. While much can be learned from visual inspection of the surfaces, other insights require actual calculation. To investigate the interplay between the vibrational modes and electronic transitions, we calculate the vibrational energies, vibrational

wavefunctions and their overlaps, and the linear absorption spectra associated with each considered mode. For these tasks, we employ our newly developed method,[61] which accepts potentials of polynomial form, thus going beyond the limitations of the standard harmonic approximation and offering much more flexibility than the analytically solvable Morse potential, which is usually the next-level method when anharmonicities are important.

For simplicity, we reduce the problem to one dimension, by only considering the most important coordinate. The resulting potential energy curve is then fitted to a polynomial using the polyfit function in Matlab, and the fitted potential is used in the above method. Convergence of the first 10 vibrational levels with respect to the degree of the fitted polynomial, required some additional potential energy single-point calculations, more details can be found in the supplementary information.

Results

While the PESs and EESs shed light on the dynamical fluctuations of the site-energies due to the intermolecular modes, it is interesting to compare to the static contribution of the residues. We therefore start this Section by looking at the effect the residues have on the BChl excitation energies by virtue of their presence. Next, we present the PESs and EESs and lastly the results from the vibrational analysis.

Static Contributions

The static energy shift induced by the presence of the residue is found by subtracting the energy of the isolated BChls from those of the BChl-residue complexes with unaltered geometries, i.e. only hydrogens have been optimised. The excitation energies and energy differences between the bare BChl and the ligated BChl can be found in Table 1, as well as the moduli of the transition dipole moments (TDMs) and the oscillator strengths. Fortunately, the TD-DFT excitation energies of the isolated BChl units (304, 305 and 308) agree

well with our previous, more accurate calculations (1.60, 1.63, 1.65 versus 1.66, 1.68, 1.70 eV, respectively), apart from the usual underestimation inherent to DFT. Also, the energy difference between the isolated and H-bonded BChl unit 304, is about the same for both TD-DFT and MS-RASPT2/2-roots-SA-RASSCF.

Interestingly, there is a clear distinction between the effect of the axial ligands and the H-bonded residues on both the energies and the TDMs/oscillator strengths. The axial ligands lower the excitation energy by 16-45 meV and increase oscillator strengths by 0.012-0.060. The H-bonded residues had the opposite effect; excitation energies were increased by 3-25 meV, while oscillator strengths were reduced by 0.002-0.008.

Potential Energy Surfaces

The MS-RASPT2/2-roots-SA-RASSCF method and TD-DFT were found to be in good agreement, particularly for geometries close to the starting structure. The comparison was made for the BChl-tyrosine complex and can be found in the supplementary information. The ground state and optically-accessible excited state PESs of all six considered modes, calculated with TD-DFT, are depicted in Figure 5.

H-bonded Residues

The PESs for the H-bonded residues are qualitatively the same, assuming lopsided single-well shapes, and not double-wells, in the proton shuttle coordinate, clearly indicating that the proton favours the residue side over the BChl side. The acetyl rotation coordinate has only a small effect on the potential energies for the range of dihedral angles we restricted the study to. The effect of the acetyl rotation is only visible to the naked eye for large displacements of the proton towards the BChl.

Histidine Residue

In contrast, the two coordinates in the BChl-histidine complex, the postition of the Mg and the histidine along their displacement vector, are equally important for the potential energies, and have a high degree of interdependence. In the PES, see Fig 5d, there is a shallow valley for the configurations where the Mg-histidine distance is approximately constant, whereas when the distance decreases the potential energy steeply rises. When the Mg and the histidine move apart, there is a small increase in potential energy, which is likely associated with pulling the Mg underneath the MCR plane.

Methionine Residue

For the methionine complexes, i.e. the neutral and the negatively charged, there is again a dominating coordinate; the vibrational mode we found in the vibrational frequency analysis. The Mg seems to have a negligible influence on this mode, resulting in an effectively one-dimensional PES with a clear anharmonic character. The presence of charge has a small effect on the curvature of the PES, particularly as the vibrational mode extends towards the BChl.

Excitation Energy Surfaces

To better resolve differences between the ground states and the excited states, we also plot excitation energy surfaces (EESs), which reveal how the site energies depend on the considered coordinates. The EESs for the BChl complexes with arginine, histidine and the neutral methionine are plotted in Figure 6, while the EESs for the remaining complexes can be found in the supplementary information. The H-bonded residues are qualitatively the same and exhibit a dip in excitation energy as the proton moves towards the BChl. This decrease is biggest for arginine, while the decrease in the tyrosine and tryptophan complexes are almost identical. However, to reach the part of configuration space where the change in excitation energy is significant, requires a lot of energy. The configuration space in the vicinity of the

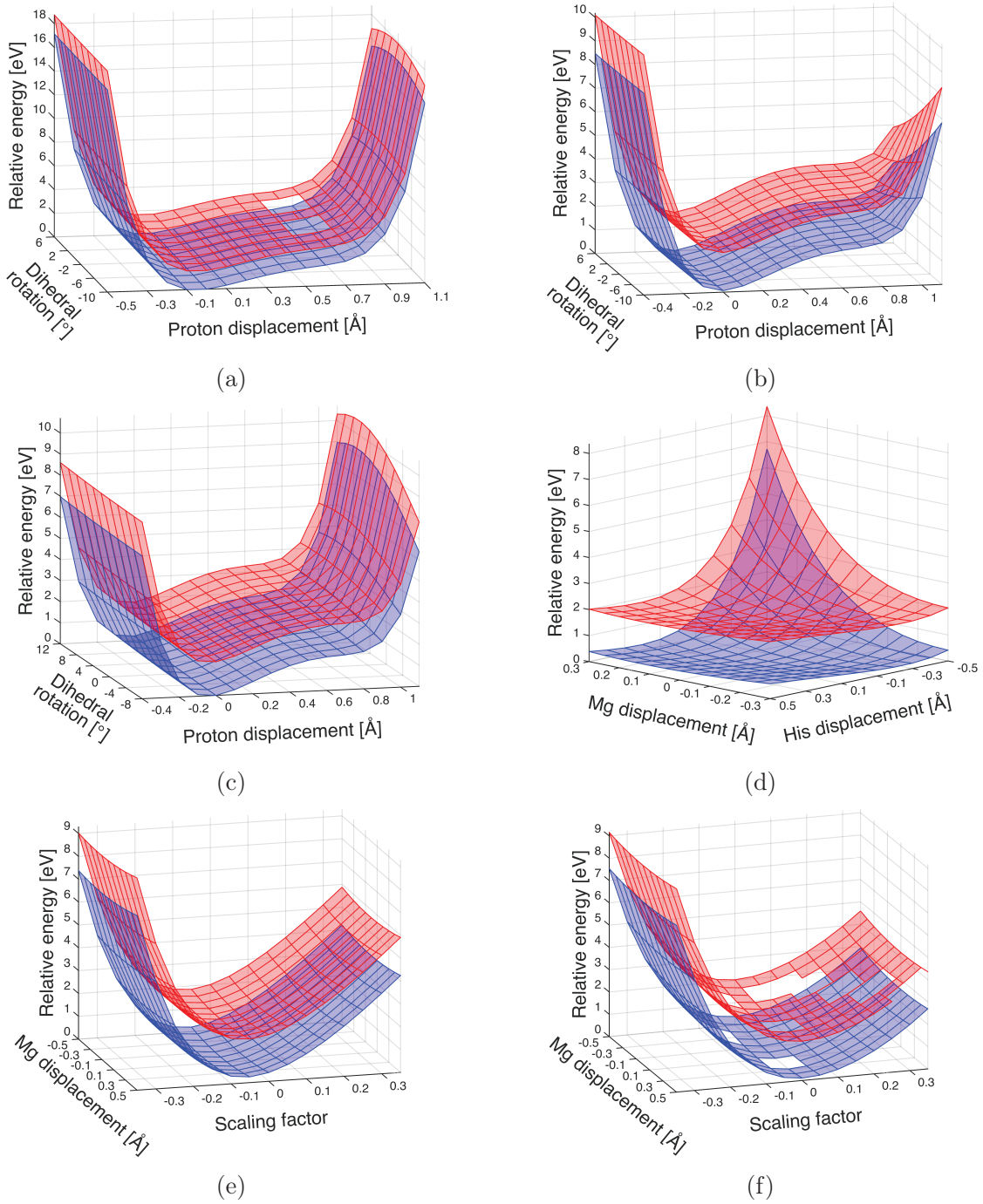

Figure 5: Potential energy surfaces of the ground state (blue) and optically-accessible excited state (red) of the BChl-residue complexes from Figure 2, with the coordinates defined in the Structures Preparation Section. The residues are: a) tyrosine b) tryptophan c) arginine d) histidine e) methionine f) negatively charged methionine. The surfaces have been shifted such that the lowest ground state energy is zero.

PESs minima corresponds to the flat parts of the EESs. Furthermore, the acetyl rotation has very little impact on the EESs. Again, the changes are smaller for the tyrosine and tryptophan complexes than for the arginine complex.

For the axial ligands, the EESs are exceptionally flat. The BChl-histidine complex shows a slightly higher excitation energy when the Mg and the histidine are at the closest, but moving them 1.6 Å further apart only results in a change in the excitation energy of less than 0.02 eV. This is in accordance with our previous study which showed that the Mg orbitals hardly participated in the excitation. For the methionine complexes, it turned out that the vibrational mode on the methionine was slightly more important for the excitation energy than the Mg coordinate. The addition of charge did not seem to change the overall picture, however, this particular system was especially difficult to calculate with our chosen energy evaluation method, which resulted in an erratic, irregular surface.

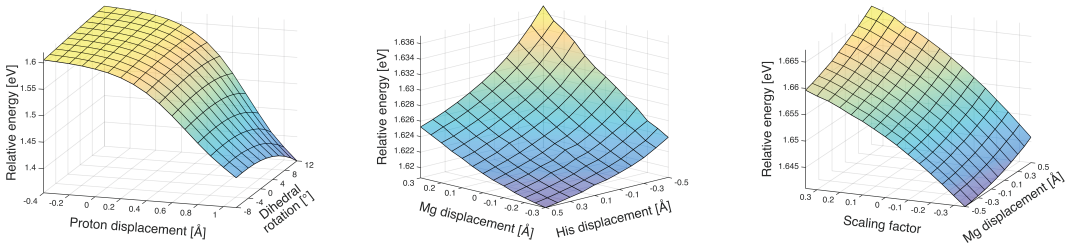

(a) (b) (c)

Figure 6: Excitation energy surfaces of the ground to first optically-excited state transition for the a) BChl-arginine complex b) BChl-histidine complex and c) BChl-methionine complex. The surfaces are computed as the difference between the ground and excited state energies in Figure 5 and make it possible to see the small differences between the ground and excited state PESs. To our surprise, the EESs are rather flat and are hardly affected by the coordinates we considered. The remaining EESs, which contain no new features compared to the ones presented here, can be found in the Supplementary Information.

Vibrational Analysis

Since there is a dominating coordinate in each of the PESs, mapping the systems to one dimension is straightforward. For the H-bonded residues this means we only take the potential energy curve of the shuttling coordinate, leaving the dihedral angle unaltered. For the

Table 1: Excitation Energies, Oscillator Strengths, Transition Dipole Moments of LH2 BChls w/ and w/o axial ligands or H-bonded residues, computed with TD-DFT

BChl #	residue type	excitation energy (eV)	energy difference	oscillator strength	transition dipole moment modulus (eÅ)
304	-	1.5990	-	0.3328	1.5435
304	Tyr	1.5821	-0.0169	0.3451	1.5800
304	His	1.6241	0.0251	0.3253	1.5142
305	-	1.6332	-	0.3425	1.5494
305	Trp	1.6171	-0.0161	0.3670	1.6118
308	-	1.6473	-	0.3400	1.5370
308	Arg	1.6024	-0.0449	0.4004	1.6913
308	Met	1.6549	0.0076	0.3383	1.5296
308	Met^-	1.6502	0.0029	0.3480	1.5536

methionine case, we disregard the Mg coordinate, and keep the Mg at the crystal structure position. In the BChl-histidine complex, the dominant mode is the His-Mg distance, however, the potential well is too shallow for reasonable/sensible values of His and Mg displacements, prohibiting a meaningful analysis of this vibrational mode.

For the neutral and negatively charged BChl-methionine complexes, we encountered problems with overfitting, which is why these two systems were only fitted to a sixth order polynomial, whereas the H-bonded residue complexes were fitted to a sixteenth order polynomial, the coefficients can be found in Table S1. The vibrational energy levels of the ground and excited states of the intermolecular modes are found in Table S2. It is clear from the initially decreasing, but later increasing, energy spacings of the H-bonded residue systems that a harmonic oscillator or a Morse oscillator description would be inadequate for the considered systems, since these methods give equidistant and monotonically decreasing energy spacings, respectively. As perhaps could have been anticipated by inspection of the PES figures, there is very little difference between the vibrational levels in the electronic ground state and excited state. Additionally, there is practically no displacement between the surfaces, which results in negligible overlaps between states with unlike vibrational quantum numbers, and near-complete overlaps between states with like vibrational quantum numbers. Combined with the fact that the energy gaps are much larger than the thermal energy at room tem-

perature (25.7 meV), meaning that only the zeroth vibrational level will be populated, the linear absorption spectra of the considered modes will consist of single peaks corresponding to the g0-e0 transitions, see Fig S3 in the supplementary information.

As a rough estimate of the timescale of the various modes (excluding the BChl-histidine complex), we calculate their vibrational periods by approximating them as harmonic oscillators, see the supplementary information. We find that all periods of vibration lie in the range 7-12 fs, but expect the histidine mode to be slower since it is more affected by the motion of the entire protein. A molecular dynamics simulation would be the suggested method to shed more light on the timescale of the BChl-histidine dynamics.

Discussion

The fact that the axial ligands and H-bonded residues were found to have opposite effects on both the energies and TDMs/oscillator strengths, could have important implications for the future design of artificial systems. For example, it is possible to envision an artifical antenna system where the BChl units are more loosely bound by the histidine residues, and therefore, in the absence of any other effect, absorbs at longer wavelengths (smaller excitation energy). However, more work is needed to ascertain if this is a general trend in natural light-harvesting systems.

The magnitude of these static contributions is quite small, which, combined with the opposite sign, results in an even smaller cumulative effect of the residues on the BChl site-energies. Furthermore, the EESs revealed that also geometrical variations in the intermolecular region had little impact on the excitation energies. However, we did not consider the possible combined effect of both the axial and H-bonded ligand, which, depending on their mutual dynamics, could enhance or diminish the overall change in excitation energy.

It is important to note, however, that even though we found surprisingly small static and dynamic contributions induced by the protein residues, it does not mean that large changes

in site-energies can not be associated with these ligands. This is because we only considered the BChls with and without the residues as taken directly from the crystal structure. The residues may also have a big effect on the BChl conformations and thus induce changes in the site-energy. This has not been accounted for in our study. The use of crystal structure geometries is supported by the fact that the energies of BChls optimised in their binding pockets more closely resemble the energies of the crystal structure geometries than those of BChls optimised in vacuum.[22]

Furthermore, some of the modes had a relatively small range of motion; this was a deliberate choice since longer displacements would likely have to be considered in conjunction with a larger environment, to account for steric hindrance and other effects.

Compared to the experimental work by Kjær et al. on the Soret band absorption of gas phase chlorophylls (Chls) with an axially bound, negatively charged carboxylate, we find a much lower energy shift for the neutral histidine and methionine ligands, as also expected by the authors, but the shifts also have opposite signs. Although the systems differ in many aspects, the most plausible explanation is perhaps that geometry changes of the BChl have been neglected. The authors also suggest that the large redshift could be purely an electrostatic effect, but the results from our BChl-methionine and BChl-methionine$^-$ complexes are almost the same, which indicates that the addition of a negative charge on the residue has a negligible effect for the BChl excitation energies.

Through our vibrational analysis we found that the electronic transitions are essentially uncoupled to the considered intermolecular vibrational modes. We therefore do not expect the studied modes to be essential components of a spectral density, nor do we believe that they should be treated explicitly in reduced density matrix models. Thus, an explanation for the large electron-phonon coupling[62] in LH2 must be found elsewhere.

While narrowing the investigation to the intermolecular region offers a more intuitive picture of which modes are important, the disadvantage is that the full effect of the environment is difficult to obtain. As such, it can serve as a complementary method to the normal

mode analysis and MD methods by providing detailed mechanistic insight of specific modes. Thus, the approach is more geared towards understanding the underlying mechanisms than reproducing spectra. If certain modes are deemed important for the energy transfer, they can, however, be incorporated in the spectral density by finding the electron-vibrational coupling via the harmonic approximation or, if the mode is anharmonic, consider the modes explicitly in reduced density matrix approaches.

Summary and Conclusions

In this paper, we have studied the effect of nearby protein residues on the ground- and excited state energies of BChls taken from the crystal structure of LH2. Using TD-DFT, we map out two-dimensional potential energy surfaces and excitation energy surfaces of selected intermolecular modes between the BChls and adjacent protein residues. The shapes of these surfaces reveal how the BChl energies are modulated by geometrical fluctuations in the region connecting the BChls with the protein environment. To our surprise, the excitation energies are highly robust against the geometrical variations of the considered modes. Moreover, through a vibrational analysis, we find the $S_0 - S_1$ optical transition to be practically uncoupled to the vibrations of the intermolecular modes.

By comparing to the energies of the corresponding isolated BChls, we find the static contribution to the excitation energy associated with the mere presence of the protein residue, i.e. disregarding induced geometry changes. Also these energy shifts are rather small. In our opinion, the large shifts in absorption seen between LH2 and LH3 can therefore not be explained solely by the presence/absence of a particular protein residue, but other effects induced by the residue or the entire binding pocket, such as for example geometry distortion, must be considered to properly account for these shifts. Work in this direction is in progress.

Interestingly, the axially ligated residues and H-bonded residues had diametrically opposite effects on both the excitation energies and the oscillator strengths, when they were

added to the isolated BChl. If this holds true for general light-harvesting systems, it could become an important design principle for artificial systems.

Supplementary Information

The supplementary information material contains a comparison of the TD-DFT and MS-RASPT2/2-roots-SA-RASSCF methods, additional excitation energy surfaces not included in the main text, the vibrational analysis results, the xyz starting structures of all the BChl-residue systems and more information on the vibrational mode on methionine that we used as one of the degrees of freedom in the main text.

Acknowledgements

TH is grateful for financial support from the Lundbeck Foundation. All calculations were conducted using the resources available at the Danish Center for Scientific Computing at Copenhagen University. The Center for Exploitation of Solar Energy is acknowledged for providing computational resources.

References

(1) Pullerits, T.; Sundström, V. Photosynthetic light-harvesting pigment-protein complexes: Toward understanding how and why. *Acc. Chem. Res.* **1996**, *29*, 381–389.

(2) Fleming, G. R.; van Grondelle, R. Femtosecond spectroscopy of photosynthetic light-harvesting systems. *Curr. Opin. Struct. Biol.* **1997**, *7*, 738–748.

(3) Hu, X.; Ritz, T.; Damjanovic, A.; Autenrieth, F.; Schulten, K. Photosynthetic apparatus of purple bacteria. *Q. Rev. Biophys.* **2002**, *35*, 1–62.

(4) Ferretti, M.; Duquesne, K.; Sturgis, J. N.; van Grondelle, R. Ultrafast excited state

processes in Roseobacter denitrificans antennae: comparison of isolated complexes and native membranes. *Phys. Chem. Chem. Phys.* **2014**, *16*, 26059–26066.

(5) Romero, E.; Augulis, R.; Novoderezhkin, V. I.; Ferretti, M.; Thieme, J.; Zigmantas, D.; van Grondelle, R. Quantum coherence in photosynthesis for efficient solar-energy conversion. *Nat. Phys.* **2014**, *10*, 676–682.

(6) Fuller, F. D.; Pan, J.; Gelzinis, A.; Butkus, V.; Senlik, S. S.; Wilcox, D. E.; Yocum, C. F.; Valkunas, L.; Abramavicius, D.; Ogilvie, J. P. Vibronic coherence in oxygenic photosynthesis. *Nat. Chem.* **2014**, *6*, 706–711.

(7) Engel, G. S.; Calhoun, T. R.; Read, E. L.; Ahn, T.-K.; Mancal, T.; Cheng, Y.-C.; Blankenship, R. E.; Fleming, G. R. Evidence for wavelike energy transfer through quantum coherence in photosynthetic systems. *Nature* **2007**, *446*, 782–786.

(8) Lee, H.; Cheng, Y.-C.; Fleming, G. R. Coherence dynamics in photosynthesis: protein protection of excitonic coherence. *Science* **2007**, *316*, 1462–1465.

(9) Chin, A. W.; Huelga, S. F.; Plenio, M. B. Coherence and decoherence in biological systems: principles of noise-assisted transport and the origin of long-lived coherences. *Phil. Trans. R. Soc. A* **2012**, *370*, 3638–3657.

(10) Kassal, I.; Aspuru-Guzik, A. Environment-assisted quantum transport in ordered systems. *New J. Phys.* **2012**, *14*, 53041.

(11) Anda, A.; Hansen, T.; Vico, L. D. Multireference excitation energies for bacteriochlorophylls a within light harvesting system 2. *J. Chem. Theory Comput.* **2016**, *12*, 1305–1313.

(12) Reimers, J. R.; Biczysko, M.; Bruce, D.; Coker, D. F.; Frankcombe, T. J.; Hashimoto, H.; Hauer, J.; Jankowiak, R.; Kramer, T.; Linnanto, J.; et al., Challenges

facing an understanding of the nature of low-energy excited states in photosynthesis. *Biochim. Biophys. Acta* **2016**, *1857*, 1627–1640.

(13) Chorosajev, V.; Rancova, O.; Abramavicius, D. Polaronic effects at finite temperatures in the B850 ring of the LH2 complex. *Phys. Chem. Chem. Phys.* **2016**, *18*, 7966–7977.

(14) Curutchet, C.; Mennucci, B. Quantum chemical studies of light harvesting. *Chem. Rev.* **2017**, *117*, 294–343.

(15) Jurinovich, S.; Curutchet, C.; Mennucci, B. The Fenna–Matthews–Olson protein revisited: A fully polarizable (TD)DFT/MM description. *Chem. Phys. Chem.* **2014**, *15*, 3194–3204.

(16) Jurinovich, S.; Viani, L.; Curutchet, C.; Mennucci, B. Limits and potentials of quantum chemical methods in modelling photosynthetic antennae. *Phys. Chem. Chem. Phys.* **2015**, *17*, 30783–30792.

(17) Daday, C.; Curutchet, C.; Sinicropi, A.; Mennucci, B.; Filippi, C. Chromophore–protein coupling beyond nonpolarizable models: understanding absorption in green fluorescent protein. *J. Chem. Theory Comput.* **2015**, *11*, 4825–4839.

(18) Rosnik, A. M.; Curutchet, C. Theoretical characterization of the spectral density of the water-soluble chlorophyll-binding protein from combined quantum mechanics/molecular mechanics molecular dynamics simulations. *J. Chem. Theory Comput.* **2015**, *11*, 5826–5837.

(19) van der Vegte, C. P.; Prajapati, J. D.; Kleinekathöfer, U.; Knoester, J.; Jansen, T. L. C. Atomistic modeling of two-dimensional electronic spectra and excited-state dynamics for a light harvesting 2 complex. *J. Phys. Chem. B* **2015**, *119*, 1302–1313.

(20) Lee, M. K.; Coker, D. F. Modeling electronic-nuclear interactions for excitation energy

transfer processes in light-harvesting complexes. *J. Phys. Chem. Lett.* **2016**, *7*, 3171–3178.

(21) Zheng, F.; Jin, M.; Mančal, T.; Zhao, Y. Study of electronic structures and pigment–protein interactions in the reaction center of thermochromatium tepidum with a dynamic environment. *J. Phys. Chem. B* **2016**, *120*, 10046–10058.

(22) König, C.; Neugebauer, J. Protein effects on the optical spectrum of the Fenna–Matthews–Olson complex from fully quantum chemical calculations. *J. Chem. Theory Comput.* **2013**, *9*, 1808–1820.

(23) Artiukhin, D. G.; Jacob, C. R.; Neugebauer, J. Excitation energies from frozen-density embedding with accurate embedding potentials. *J. Chem. Phys.* **2015**, *142*, 234101.

(24) Jacob, C. R.; Neugebauer, J. Subsystem density-functional theory. *Wiley Interdiscip. Rev. Comput. Mol. Sci.* **2014**, *4*, 325–362.

(25) Renger, T.; Klinger, A.; Steinecker, F.; am Busch, M.; Numata, J.; Müh, F. Normal mode analysis of the spectral density of the Fenna–Matthews–Olson light-harvesting protein: how the protein dissipates the excess energy of excitons. *J. Phys. Chem. B* **2012**, *116*, 14565–14580.

(26) Jing, Y.; Zheng, R.; Li, H.-X.; Shi, Q. Theoretical study of the electronic–vibrational coupling in the Qy states of the photosynthetic reaction center in purple bacteria. *J. Phys. Chem. B* **2012**, *116*, 1164–1171.

(27) MacGowan, S. A.; Senge, M. O. Contribution of bacteriochlorophyll conformation to the distribution of site-energies in the {FMO} protein. *Biochim. Biophys. Acta* **2016**, *1857*, 427–442.

(28) Kjæ r, C.; Stockett, M. H.; Pedersen, B. M.; Nielsen, S. B. Strong impact of an axial

ligand on the absorption by chlorophyll a and b pigments determined by gas-phase ion spectroscopy experiments. *J. Phys. Chem. B* **2016**, *120*, 12105–12110.

(29) Ferretti, M.; Novoderezhkin, V. I.; Romero, E.; Augulis, R.; Pandit, A.; Zigmantas, D.; van Grondelle, R. The nature of coherences in the B820 bacteriochlorophyll dimer revealed by two-dimensional electronic spectroscopy. *Phys. Chem. Chem. Phys.* **2014**, *16*, 9930–9939.

(30) Bednarczyk, D.; Dym, O.; Prabahar, V.; Peleg, Y.; Pike, D. H.; Noy, D. Fine tuning of chlorophyll spectra by protein-induced ring deformation. *Angew. Chem. Int. Ed.* **2016**, *55*, 6901–6905.

(31) Papiz, M. Z.; Prince, S. M.; Howard, T.; Cogdell, R. J.; Isaacs, N. W. The structure and thermal motion of the B800-850 LH2 complex from Rps.acidophila at 2.0A resolution and 100K: new structural features and functionally relevant motions. *J. Mol. Biol.* **2003**, *326*, 1523–1538.

(32) Cogdell, R. J.; Howard, T. D.; Isaacs, N. W.; McLuskey, K.; Gardiner, A. T. Structural factors which control the position of the Qy absorption band of bacteriochlorophyll a in purple bacterial antenna complexes. *Photosynth. Res.* **2002**, *74*, 135–141.

(33) McLuskey, K.; Prince, S. M.; Cogdell, R. J.; Isaacs, N. W. The crystallographic structure of the B800-820 LH3 light-harvesting complex from the purple bacteria rhodopseudomonas acidophila strain 7050†. *Biochemistry* **2001**, *40*, 8783–8789.

(34) Alia, A.; Matysik, J.; de Boer, I.; Gast, P.; van Gorkom, H. J.; de Groot, H. J. M. Heteronuclear 2D (1H-13C) MAS NMR resolves the electronic structure of coordinated histidines in light-harvesting complex II: Assessment of charge transfer and electronic delocalization effect. *J. Biomol. NMR* **2004**, *28*, 157–164.

(35) Alia, A.; Matysik, J.; Soede-Huijbregts, C.; Baldus, M.; Jan Raap,; Lugtenburg, J.; Gast, P.; Gorkom, V.; Hoff, A. J.; and Huub J. M. de Groot, Ultrahigh field MAS NMR

dipolar correlation spectroscopy of the histidine residues in light-harvesting complex II from photosynthetic bacteria reveals partial internal charge transfer in the B850/His complex. *J. Am. Chem. Soc.* **2001**, *123*, 4803–4809.

(36) Wawrzyniak, P. K.; Alia, A.; Schaap, R. G.; Heemskerk, M. M.; de Groot, H. J. M.; Buda, F. Protein-induced geometric constraints and charge transfer in bacteriochlorophyll-histidine complexes in LH2. *Phys. Chem. Chem. Phys.* **2008**, *10*, 6971–6978.

(37) Fenna, R. E.; Matthews, B. W. Chlorophyll arrangement in a bacteriochlorophyll protein from Chlorobium limicola. *Nature* **1975**, *258*, 573–577.

(38) Matthews, B.; Fenna, R.; Bolognesi, M.; Schmid, M.; Olson, J. Structure of a bacteriochlorophyll a-protein from the green photosynthetic bacterium Prosthecochloris aestuarii. *J. Mol. Biol.* **1979**, *131*, 259–285.

(39) Fowler, G. J. S.; Visschers, R. W.; Grief, G. G.; van Grondelle, R.; Hunter, C. N. Genetically modified photosynthetic antenna complexes with blueshifted absorbance bands. *Nature* **1992**, *355*, 848–850.

(40) Runge, E.; Gross, E. K. U. Density-functional theory for time-dependent systems. *Phys. Rev. Lett.* **1984**, *52*, 997–1000.

(41) Dreuw, A.; Head-Gordon, M. Single-reference ab initio methods for the calculation of excited states of large molecules. *Chemical Reviews* **2005**, *105*, 4009–4037.

(42) Casida, M.; Huix-Rotllant, M. Progress in time-dependent density-functional theory. *Annual Review of Physical Chemistry* **2012**, *63*, 287–323.

(43) Roos, B. O.; Taylor, P. R.; Siegbahn, P. E. A complete active space SCF method (CASSCF) using a density matrix formulated super-CI approach. *Chemical Physics* **1980**, *48*, 157 – 173.

(44) Malmqvist, P.-Å.; Pierloot, K.; Shahi, A. R. M.; Cramer, C. J.; Gagliardi, L. The restricted active space followed by second-order perturbation theory method: Theory and application to the study of CuO2 and Cu2O2 systems. *The Journal of Chemical Physics* **2008**, *128*, 204109.

(45) Roos, B.; Andersson, K.; Fülscher, M.; Malmqvist, P.-Å.; Serrano-Andrés, L.; Pierloot, K.; Merchán, M. In *Advances in Chemical Physics: New Methods in Computational Quantum Mechanics*; Prigogine, I., Rice, S., Eds.; John Wiley & Sons: New York, 1996; pp 219–332.

(46) Finley, J.; Malmqvist, P.-Å.; Roos, B. O.; Serrano-Andrés, L. The multi-state CASPT2 method. *Chemical Physics Letters* **1998**, *288*, 299 – 306.

(47) Roos, B. O.; Lindh, R.; Malmqvist, P.-Å.; Veryazov, V.; Widmark, P.-O. Main group atoms and dimers studied with a new relativistic ANO basis set. *The Journal of Physical Chemistry A* **2004**, *108*, 2851–2858.

(48) Aquilante, F.; De Vico, L.; Ferré, N.; Ghigo, G.; Malmqvist, P.-Å.; Neogrády, P.; Pedersen, T. B.; Pitoňák, M.; Reiher, M.; Roos, B. O.; et al., MOLCAS 7: The next generation. *Journal of Computational Chemistry* **2010**, *31*, 224–247.

(49) Aquilante, F.; Autschbach, J.; Carlson, R. K.; Chibotaru, L. F.; Delcey, M. G.; De Vico, L.; Fernández. Galván, I.; Ferré, N.; Frutos, L. M.; Gagliardi, L.; et al., MOLCAS 8: New capabilities for multiconfigurational quantum chemical calculations across the periodic table. *Journal of Computational Chemistry* **2016**, *37*, 506–541.

(50) Hanwell, M.; Curtis, D.; Lonie, D.; Vandermeersch, T.; Zurek, E.; Hutchison, G. Avogadro: an advanced semantic chemical editor, visualization, and analysis platform. *Journal of Cheminformatics* **2012**, *4*, 17.

(51) Stewart, J. Optimization of parameters for semiempirical methods V: Modification of

NDDO approximations and application to 70 elements. *Journal of Molecular Modeling* **2007**, *13*, 1173–1213.

(52) Frisch, M. J.; Trucks, G. W.; Schlegel, H. B.; Scuseria, G. E.; Robb, M. A.; Cheeseman, J. R.; Scalmani, G.; Barone, V.; Mennucci, B.; Petersson, G. A.; et al., Gaussian 09 Revision D.01. Gaussian, Inc.: Wallingford, CT, 2009.

(53) Aidas, K.; Angeli, C.; Bak, K. L.; Bakken, V. r.; Bast, R.; Boman, L.; Christiansen, O.; Cimiraglia, R.; Coriani, S.; Dahle, P. l.; et al., The Dalton quantum chemistry program system. *Wiley Interdiscip. Rev. Comput. Mol. Sci.* **2014**, *4*, 269–284.

(54) Krishnan, R.; Binkley, J. S.; Seeger, R.; Pople, J. A. Self-consistent molecular orbital methods. XX. A basis set for correlated wave functions. *The Journal of Chemical Physics* **1980**, *72*, 650–654.

(55) McLean, A. D.; Chandler, G. S. Contracted Gaussian basis sets for molecular calculations. I. Second row atoms, Z=11-18. *The Journal of Chemical Physics* **1980**, *72*, 5639–5648.

(56) Clark, T.; Chandrasekhar, J.; Spitznagel, G. W.; Schleyer, P. V. R. Efficient diffuse function-augmented basis sets for anion calculations. III. The 3-21+G basis set for first-row elements, Li-F. *Journal of Computational Chemistry* **1983**, *4*, 294–301.

(57) Tanaka, M.; Katouda, M.; Nagase, S. Optimization of RI-MP2 auxiliary basis functions for 6-31G** and 6-311G** basis sets for first-, second-, and third-row elements. *Journal of Computational Chemistry* **2013**, *34*, 2568–2575.

(58) Adamo, C.; Barone, V. Toward reliable density functional methods without adjustable parameters: The PBE0 model. *J. Chem. Phys.* **1999**, *110*, 6158.

(59) List, N. H.; Curutchet, C.; Knecht, S.; Mennucci, B.; Kongsted, J. Toward reliable

prediction of the energy ladder in multichromophoric systems: A benchmark study on the FMO light-harvesting complex. *J. Chem. Theory Comput.* **2013**, *9*, 4928–4938.

(60) Davidson, E. R. The iterative calculation of a few of the lowest eigenvalues and corresponding eigenvectors of large real-symmetric matrices. *Journal of Computational Physics* **1975**, *17*, 87 – 94.

(61) Anda, A.; De Vico, L.; Hansen, T.; Abramavičius, D. Absorption and fluorescence lineshape theory for polynomial potentials. *J. Chem. Theory Comput.* **2016**, *12*, 5979–5989.

(62) Freiberg, A.; Rätsep, M.; Timpmann, K. o.; Trinkunas, G.; Woodbury, N. W. Self-trapped excitons in LH2 antenna complexes between 5 K and ambient temperature. *J. Phys. Chem. B* **2003**, *107*, 11510–11519.

Table of Contents Graphic

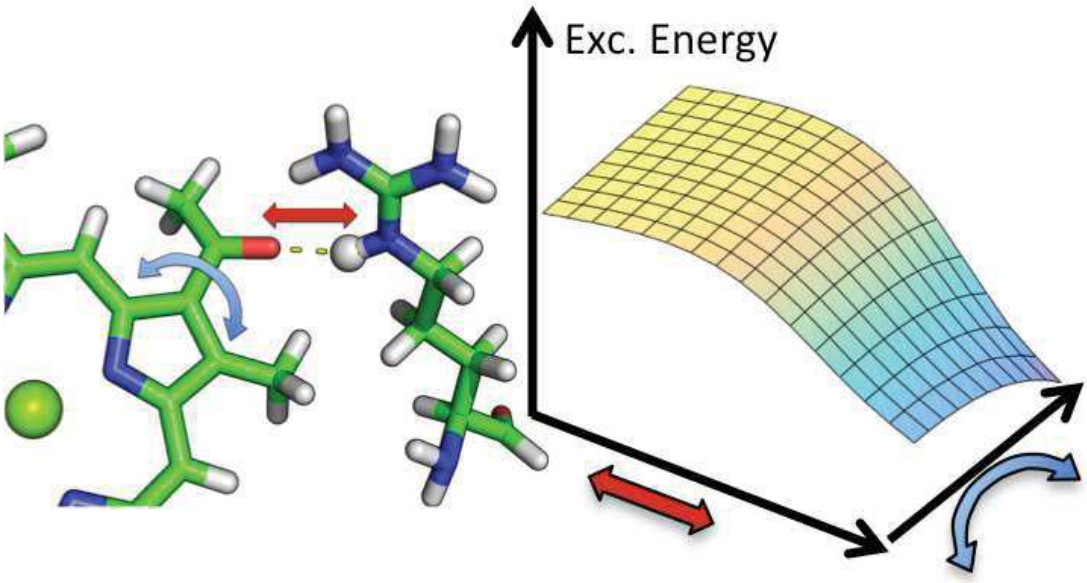

Figure 7